 doi:10.20944/preprints201811.0619.v1

Type of the Paper: Article

Energy and Entropy in Turbulence Decompositions

Václav Uruba [1,2,*]

[1] Institute of Thermomechanics, ASCR, v.v.i., Dolejškova 5, Praha 8, CR; uruba@it.cas.cz
[2] University of West Bohemia, Faculty of Mechanical Engineering, Department of Power System Engineering, Universitní 8, Plzeň, CR; uruba@kke.zcu.cz
* Correspondence: uruba@it.cas.cz; Tel.: +420-266 053 414

Abstract: The role of energy and entropy in decomposition of turbulent velocity flow-fields is to be shown in the paper. The decomposition methods based on energy concept are taken into account, namely the Proper Orthogonal Decomposition (POD) and its extension Bi-Orthogonal Decomposition (BOD). Entropy motivated view on the decomposed modes could offer new possibilities in the modes physical interpretation and in Reduced Order Modelling (ROM) strategy efficiency evaluation.

Keywords: turbulence ; coherent structures ; decomposition ; energy ; entropy

1. Introduction

Turbulence in fluids is a highly dynamical phenomenon which is characterized by complex topology. The duality of randomness and coherency is typical for this phenomenon. It could be identified as a blend of emergence of coherent structures and fully random behavior, it is extremely important to distinguish these two complementary parts. In this difficult task the quantities as "coherency" and "entropy" play very important role.

The turbulent flow-field is populated by coherent structures, see e.g. [1]. These are vortices very often of various sizes, positions and orientations in space with complex dynamics. To study this complicated phenomenon various strategies are used. Classical approach is to identify the individual structures and explore theirs evolution in time and space. This is a very exhausting task, so statistical tools are to be applied. The basic method of the coherent structures identification remains Proper Orthogonal Decomposition (hereinafter POD) [2] or its generalized version Bi-Orthogonal Decomposition (hereinafter BOD) [3].

The turbulent data is available in the form of snapshots very often. A snapshot shows the instantaneous spatial distribution of a given physical quantity characterizing the flow-field. Instantaneous velocity vector-fields are used usually. However, the methods could work with any physical quantity whose distribution in space could be determined, it could be e.g. vorticity, pressure or concentration of a contaminant. The input data could come from experiment, e.g. from Particle Image Velocimetry (PIV) or other optical methods or from mathematical modelling, Direct Numerical Simulation or Large Eddy Simulation.

The decomposition methods are based on idea of the Hilbert space, which is defined by all snapshots forming a natural basis of the Hilbert space, see [4]. The goal of the decomposition methods is to find another appropriate base with a distinct physical meaning. The POD and BOD methods are looking for an orthonormal basis maximizing the dynamic data variance. Variance could be linked to fluctuations energy. Orthogonality condition implies decorrelation of the modes, which is the necessary condition for statistical independence, but not the sufficient one, see [5].

The decomposition methods based on POD could provide an efficient basis for Reduced Order Modelling (herein after ROM) of the complex system dynamics. Searching process for the optimal basis covering maximal fluctuating kinetic energy of the real system dynamics could be considered as information compression process, if the information describes spatio-temporal behavior of the system. However, not any information could be compressed efficiently, efficiency of this process is to be assessed. More coherent system behavior, more efficient the compression could be. Efficiency

of the compression could be assessed with help of system information entropy evaluation. More entropy, less efficient the compression process could be. Information about entropy is distributed in time and space as the energy is. Global information is provided by total or global entropy.

In the presented paper the POD and BOD methods will be introduced in context of coherency evaluation with help of entropy definition on top of it.

2. Historical notes

The POD method has applications in almost any scientific field where extended dynamical systems are involved. This fact accounts for the frequency of POD's discovery. We could follow this process on the time axis: first Pearson in 1901 [6], then Hotelling in 1933 [7], Kosambi in 1943 [8], Loeve in 1945 [9], Karhunen in 1946 [10], Pougachev in 1953 [11] and Obukhov in 1954 [12]. All of them have been credited with independent discovery of POD under one of its many titles, which include Principle Component Analysis, Karhunen-Loeve Decomposition or Expansion, Principle Factor Analysis, Hotelling Transform, and Collective Coordinates. Details could be found e.g. in [13].

Recently, the POD has been widely used in studies of turbulence, as appropriate data is at our disposal eventually. Historically, the POD method was introduced in the context of turbulence by Lumley in 1967 [2] as an objective definition of what was previously called big eddies and which is now widely known as coherent structures.

The POD is considered to be a natural idea to replace the usual Fourier decomposition in nonhomogeneous directions. Adrian [14] considers the POD as inhomogeneous filtering applied on the flow data in the framework of the Large Eddy Simulation method. The classical homogeneous filtering, using the Gaussian filter for example, is inconsistent with the fact that the turbulent eddies increase in size as they move away from the wall. This problem can be addressed by using the method of POD to construct low-pass filters that are inhomogeneous in one or more direction. The POD provides an optimal set of base functions for an ensemble of data in the sense that it is the most efficient way of extracting the most energetic components of an infinite dimensional process with only a few modes.

The POD method is optimal in sense that the series of eigenmodes converges more rapidly (in quadratic mean) than any other representation. Convergence is very fast in the flows in which large coherent structures contain a major fraction of the total kinetic energy. As an example the pseudo-periodical vortex streets in wakes or strong shear layers could be mentioned – see the example in Chapter 5.

An advantage of the method is its objectivity and lack of bias. Given a realization of an in-homogenous, energy-integrable velocity field, it consists of projecting the random field on a candidate structure, and selecting the structure which maximizes the projection in quadratic mean. In other words, we are interested in the structure which is the best correlated with the random, energy-integrable field. More precisely, we are given an ensemble of realizations of the field, the purpose is to find the structure which is the best correlated with all the elements of the ensemble. Thus we want to maximize a statistical measure of the magnitude of the projection, which can be given by the mean square of its absolute value.

The calculus of variations reduces this problem of maximization to a Fredholm integral equation of the first kind whose symmetric kernel is the autocorrelation matrix, see e.g. [4]. The properties of this integral equation are given by Hilbert-Schmidt theory. There is denumerable set of eigenfunctions (structures). The eigenfunctions form a complete orthogonal set, which means that the random field can be reconstructed. The coefficients are uncorrelated and their mean square values are the eigenvalues themselves. The Kernel can be expanded in a uniformly and absolutely convergent series of the eigenfunctions and the turbulent kinetic energy is the sum of the eigenvalues. Thus every structure makes an independent contribution to the kinetic energy and Reynolds stress.

3. Decomposition methods

The existence of so-called Coherent Structures in turbulent flows is now well accepted (see e.g. [1]). Lumley [15] introduced the concept of “building blocks” (i.e. basis of non-specified functions)

Preprints (www.preprints.org) | NOT PEER-REVIEWED | Posted: 29 November 2018 doi:10.20944/preprints201811.0619.v1

based on the notion of "energetic modes" on which the velocity field is projected. The modes maximize velocity variance, i.e. kinetic energy of the process.

Extraction of deterministic features from a random, fine grained turbulent flow has been a challenging problem. Lumley proposed an unbiased technique for identifying such structures. The method consists of extracting the candidate which is the best correlated, in statistical sense, with the background velocity field. The different structures are identified with the orthogonal eigenfunctions of the decomposition theorem of probability theory. This is thus a systematic way to find organized motions in a given set of realizations of a random field.

An overview of the energy based decomposition methods could be find in [16].

3.1 Kinetic Energy Definition

Kinetic energy is a key quantity in a flow-field analysis. Specific kinetic energy is considered very often, related to a unity mass. In the theory of turbulence it is based on definition of velocity subjected to Reynolds decomposition:

$$v_i(\mathbf{x},t) = V_i(\mathbf{x}) + v_i'(\mathbf{x},t), \tag{1}$$

where v_i is the instantaneous i-th velocity component, V_i is the velocity component mean value and v_i' is its fluctuation part, $\mathbf{x}$ is position vector and t is time. The mean value is to be evaluated as an ensemble average $\langle v_i(\mathbf{x},t)\rangle$, replaced usually by the time mean value $\frac{1}{T}\int_0^T v_i(\mathbf{x},t)\,dt$, as the process is supposed to be ergodic. The T is the time interval, sufficiently long.

Then the total kinetic energy K_T could be defined as sum of mean kinetic energy K and is fluctuating kinetic energy k

$$K_T(\mathbf{x}) = \frac{1}{2}\langle v_i^2(\mathbf{x},t)\rangle = \frac{1}{2}\left(V_i^2(\mathbf{x}) + \langle v_i'^2(\mathbf{x},t)\rangle\right) = K(\mathbf{x}) + k(\mathbf{x}), \quad i=1,2,3 \tag{2}$$

The fluctuating kinetic energy k is called Turbulent Kinetic Energy (TKE):

$$k(\mathbf{x}) = \frac{1}{2}\langle v_i'^2(\mathbf{x},t)\rangle, \quad i=1,2,3 \tag{3}$$

The index i is additive, subjected to the Einstein rule in formulas (2) and (3).

From an experiment, n velocity components (typically 2 or 3) in a rectangular region can be evaluated, overall M points in space. The *i*-th component of the *j*-th point in space is $v_{ij}(t)$, corresponding position vector is $\mathbf{x}_j$, $v_{ij}'(t)$ is the velocity fluctuation. The velocity fluctuating components $v_{ij}'(t)$ could be reordered into a single state vector of velocity fluctuations $\mathbf{u}(t)$ or $u_i(t)$ in tensor notation. Now, we define the kinetic energy of the system E as a sum of energies of all detected components in all points in space:

$$E = \frac{1}{M}\sum_{j=1}^{M} k(\mathbf{x}_j) = \frac{1}{2M}\sum_{i=1}^{n}\sum_{j=1}^{M}\langle v_{ij}'^2(t)\rangle = \frac{1}{2M}\sum_{i=1}^{N_x}\langle u_i^2(t)\rangle, \quad N_x = n\cdot M \tag{4}$$

The total number of velocity components involved in the problem N_x is equal to the number of Degrees-of-Freedom, being the dimension of the state vector in the same time.

This total kinetic energy of the system is taken into account in subsequent analysis based on energy approach. Please note, that for the 2 evaluated velocity components only part of the TKE is covered by this quantity.

3.2 Proper Orthogonal Decomposition

Lumley proposed to define a coherent structure with functions of the spatial variables that have maximum energy content. That is, coherent structures are $\boldsymbol{\varphi}(\mathbf{x})$'s (or linear combinations of) which maximize the following expression

Preprints (www.preprints.org) | NOT PEER-REVIEWED | Posted: 29 November 2018 doi:10.20944/preprints201811.0619.v1

$$\frac{\left\langle \left(\boldsymbol{\varphi}(\mathbf{x}), \mathbf{u}(\mathbf{x},t)\right)^2 \right\rangle}{\left\langle \boldsymbol{\varphi}(\mathbf{x}), \boldsymbol{\varphi}(\mathbf{x}) \right\rangle}, \tag{5}$$

where the expression (f,g) denotes the inner product $\int_\Omega fg\, d\Omega$ in L^2 on the space domain Ω and the $\langle f \rangle$ is mean in time. So, if $\boldsymbol{\varphi}(\mathbf{x})$ maximizes (5), it means that if the flow-field is projected along $\boldsymbol{\varphi}(\mathbf{x})$, the average energy content is larger than if the flow-field is projected along any other structure. Then, in the space orthogonal to the evaluated $\boldsymbol{\varphi}(\mathbf{x})$ the maximization process can be repeated, and in this way a whole set of orthogonal functions $\boldsymbol{\varphi}_i(\mathbf{x})$ can be determined. The power of the POD lies in the fact that the decomposition of the flow-field in the POD eigenfunctions basis converge optimally fast in L_2-sense.

Using variation calculus it could be shown that a necessary condition for $\boldsymbol{\varphi}(\mathbf{x})$ to maximize expression (5) is that it is the solution of the following Fredholm integral equation of the second type:

$$\int_\Omega \mathbf{R}_s(\mathbf{x},\mathbf{x}')\,\boldsymbol{\varphi}(\mathbf{x}')\,d\mathbf{x}' = \lambda^2\,\boldsymbol{\varphi}(\mathbf{x}), \tag{6}$$

where Ω is the flow domain and $\mathbf{R}_s$ is the space-correlation matrix:

$$\mathbf{R}_s(\mathbf{x},\mathbf{x}') = \left\langle \mathbf{u}(\mathbf{x})\,\mathbf{u}^T(\mathbf{x}') \right\rangle = \int_T \mathbf{u}(\mathbf{x},t)\,\mathbf{u}^T(\mathbf{x}',t)\,dt. \tag{7}$$

The correlation matrix is symmetric and positive definite. According to Hilbert-Schmidt theory, the equation (6) has a denumerable set of orthogonal solutions – eigenfunctions $\boldsymbol{\varphi}_i(\mathbf{x})$ with corresponding real and positive eigenvalues λ_i.

The eigenfunctions are orthogonal and can be normalized:

$$\left(\boldsymbol{\varphi}_i, \boldsymbol{\varphi}_j\right) = \delta_{ij}. \tag{8}$$

The closure of the span of the POD eigenfunctions is equal to the set of all realizable flow-fields. Therefore any flow-field could be expressed as a linear combination of the eigenfunctions:

$$\mathbf{u}(\mathbf{x},t) = \sum_{k=1}^{\infty} a_k(t)\,\boldsymbol{\varphi}_k(\mathbf{x}). \tag{9}$$

The above given formulation represents itself the continuous variant of the POD implementation. However, this formulation is not very appropriate for direct application.

The eigenvalues λ_i^2 are related to the given mode energy, as they represent a sum of all velocity components variances.

3.3 Snapshot POD

This variant of the POD method implementation uses space instead of time correlations.

The method was proposed by Sirovich in 1987 [17]. For the snapshot POD we need a set of N_t snapshots $\mathbf{u}_i(\mathbf{x})$ of the fluctuating velocity field. The snapshots are taken at different times from a simulation

$$\mathbf{u}_k(\mathbf{x}) = \mathbf{u}(\mathbf{x},t_k). \tag{10}$$

The snapshots should be mutually linearly independent, this condition implies that $N_t \le N_x$. The maximization problem (5) can be reformulated for the snapshots

$$\frac{\frac{1}{N_t}\sum_{k=1}^{N_t}\left(\boldsymbol{\varphi}(\mathbf{x}), \mathbf{u}_k(\mathbf{x})\right)^2}{\left(\mathbf{u}_k(\mathbf{x}), \mathbf{u}_k(\mathbf{x})\right)}. \tag{11}$$

 doi:10.20944/preprints201811.0619.v1

Supposing applicability of the ergodicity hypothesis we could rewrite expression for correlation function in the following way:

$$\mathbf{R}_s(\mathbf{x},\mathbf{x}') = \lim_{k\to\infty} \sum_{k=1}^{N_t} \mathbf{u}_k(\mathbf{x})\,\mathbf{u}_k^T(\mathbf{x}'). \tag{12}$$

In this equation the time between the snapshots has to be large enough for the snapshots to be uncorrelated. The idea is now to take a finite N large enough for a reasonable approximation of $\mathbf{R}_s(\mathbf{x},\mathbf{x}')$. Substituting (12) into the Fredholm integral equation (6) results into a degenerate integral equation. Therefore the solutions are linear combinations of the snapshots:

$$\boldsymbol{\varphi}_k(\mathbf{x}) = \sum_{k=1}^{N_t} q_{ki}\mathbf{u}_k(\mathbf{x}). \tag{13}$$

Thus the problem is reduced to finding the coefficients q_{ki} of the linear combination. If we substitute (13) into the degenerated integral equation we obtain the following eigenvalue problem for the coefficients q_{ki}:

$$\mathbf{Q}\mathbf{q} = \lambda^2\mathbf{Q}, \quad Q_{ij} = \frac{1}{N_t}\left(\mathbf{u}_i(\mathbf{x}),\mathbf{u}_j(\mathbf{x})\right). \tag{14}$$

The dimension of this eigenvalue problem is equal to the number of snapshots, which is typically much lower than the dimension of the eigenvalue problem (6). The method of Sirovich uses the ergodicity hypothesis to approximate $\mathbf{R}_s$, so we can expect the POD eigenfunctions to converge to the POD eigenfunctions of the continuous formulation. In fact, the snapshot method proves equivalence of information content in space and time correlation. This fact could be utilized for analysis of both space and time structures, as the Bi-Orthogonal Decomposition does.

Please note that in snapshot POD version the number Degrees of Freedom is equal to N_t.

3.4 Bi-Orthogonal Decomposition

The Bi-Orthogonal Decomposition (BOD) represents itself an extension of the POD and technically it is a combination of POD and Snapshot POD methods. While POD analyses data in spatial domain only, the BOD performs spatio-temporal decomposition. The effective number of Degree of Freedom is now given by complexity of the process in space and time. In practice we consider N Degrees of Freedom:

$$N = \min(N_x, N_t), \tag{15}$$

as the complexity in both domains (space and time) should be equivalent.

Aubry in [3] presented the BOD as a deterministic analysis tool for complex spatiotemporal signals. First, a complete two-dimensional decomposition was performed. These decompositions were based on two-point temporal and spatial velocity correlations. A set of orthogonal spatial (Topos) and temporal (Chronos) eigenmodes are to be computed to allow the expansion of the velocity field. The BOD method analyses a deterministic space-time signal (e.g. velocity) $\mathbf{u}(\mathbf{x},t)$, which is decomposed in the following way:

$$\mathbf{u}(\mathbf{x},t) = \sum_k \lambda_k\, \overline{\boldsymbol{\varphi}_k(\mathbf{x})}\, \boldsymbol{\psi}_k(t). \tag{16}$$

The bar denotes complex conjugate, $\boldsymbol{\varphi}_k(\mathbf{x})$ are spatial eigenfunctions Topoi, $\boldsymbol{\psi}_k(t)$ are temporal eigenfunctions Chronos, λ_k^2 are the common eigenvalues. Please note that both Topos and Chronos are dimensionless and orthonormal. The only quantity with physical dimension in the right-hand side of (16) is the square root of the eigenvalue λ_k, which poses the same physical dimension as the quantity on the left-hand side. Mathematical details of the BOD method could be found in [3].

The orthogonal decomposition is optimal in sense of a fast convergence of the expansion with a small number of terms. It should be noticed that the BOD introduces a time-space separation in the velocity field expansion. While the classic orthogonal decomposition POD is based on full two-point

 doi:10.20944/preprints201811.0619.v1

space-time correlations and entails space and time-dependent eigenmodes, BOD is closer to analytical and numerical studies where the velocity field is naturally expanded over products of spatial functions and temporal functions.

Evaluation technique of the eigenfunctions uses the same mathematics as the POD does. In principle the Fredholm integral equation could be written in the two forms for space and time correlation matrices, the eigenvalues are common for both problems, but eigenfunctions differ, of course. For the time domain formulation we get the following form (compare with (6)):

$$\int_T \mathbf{R}_t(t,t')\,\boldsymbol{\psi}(t')\,dt' = \lambda^2\,\boldsymbol{\psi}(t)\,, \tag{17}$$

where correlation matrix $\mathbf{R}_t$ stands for

$$\mathbf{R}_t(t,t') = \int_\Omega \mathbf{u}(\mathbf{x},t)\,\mathbf{u}^T(\mathbf{x},t')\,d\mathbf{x}\,. \tag{18}$$

The Topoi and Chronoses are related in the following way:

$$\begin{aligned}\boldsymbol{\varphi}_k(\mathbf{x}) &= \frac{1}{\lambda_k}\sum_{i=1}^{N}\mathbf{u}(\mathbf{x},t_i)\,\boldsymbol{\psi}_k(t_i)\\ \boldsymbol{\psi}_k(t) &= \frac{1}{\lambda_k}\sum_{i=1}^{N}\mathbf{u}(\mathbf{x}_i,t)\,\boldsymbol{\varphi}_k(\mathbf{x}_i)\end{aligned} \tag{19}$$

The decomposition allows us to study energy and entropy of the fluid system as well as its dynamical behavior.

The spatial quantities characterize the distributions in space, while temporal in time. According to the developers of the BOD themselves there is no real link between BOD and POD, since they are based on fundamentally different principles. In fact, BOD can be seen as a time–space symmetric version of the Karhunen–Loeve expansion or, in other words, a combination of the classical POD and the snapshot POD. However, the main difference seems to be is the assumptions on the analyzed signal, which has to be square integrable only for the BOD, instead of square integrable, ergodic and stationary for the POD. The BOD is a more general method and the POD method should be considered as its particular case. Moreover, the BOD is not derived from an optimization problem of the mean-square projection of the signal as in POD, although the method of calculation of BOD leads also to an eigenvalue problem of a correlation operator. The geometrical interpretation in state space, especially the principal axes of the ellipsoid vanishes in the case of BOD.

Each mode consists of the energy contents (sum of energy of all local velocity components), the spatial mode (Topos) and the temporal mode (Chronos). The mode amplitude is equal to square root of energy. The modes are typically ordered according to decreasing energy content. The original series of snapshots can be fully reconstructed using the entire set of modes. Neglecting the high order modes, the low-energy random noise can be removed, which can arise in consequence of the process randomness, measurement/evaluation errors or in connection with unresolved subgrid structures in the flow.

Both Topoi and Chronoses form orthonormal bases. To study the embedded system dynamics, the Chronoses multiplied by the mode amplitude can be used to characterize the system evolution in time.

Typical high-energy modes are periodical patterns. In this case two modes are related to each periodical pattern very often shifted by a quarter of a period. For analysis of the periodical aspects of such flows the reconstruction using two such modes is adequate.

To capture the time resolution of the process in a proper way and obtain representative Chronoses, the usual rules should be followed, including Nyquist criterion. This means that the acquisition frequency should be higher than twice the maximal frequency of the process. If this condition is not kept, the frequency content of the time-dependent behavior is not reproduced properly because of masking effect of aliasing. However to study the details of the behavior in time, a much higher multiplier is necessary (5-10 instead of 2).

Preprints (www.preprints.org) | NOT PEER-REVIEWED | Posted: 29 November 2018 doi:10.20944/preprints201811.0619.v1

The modes are orthogonal and thus uncorrelated. Decorrelation of modes is the necessary condition for their independence, but generally not the sufficient. In practice for signals random in time this condition is sufficient, but for periodically time-evolved signals the condition is satisfied for two phases shifted by $\pi/2$ one relative to other. The consequence of the orthogonal feature, which is in fact nonphysical, is a problem in the physical interpretation of the individual modes. The spectra of all Chronoses are in general dense for a broad-band process.

A few characteristics are defined to characterize the decomposition results. Energy and entropy distributions in time and Euclidian space can be evaluated. Energy distributions show distributions of kinetic energy of the process. Entropy or more precisely information entropy is a measure of the uncertainty associated with underlying random process and it is connected with the compression of information using the BOD method.

In case that one of the space coordinates is chosen to be the state variable for the BOD analysis, the modes represent dynamical behavior of the process not in time but in space in a given direction . Two types of modes result, as in the classical BOD variant. One mode characterizes the system behavior for the chosen state variable (space coordinate) to be independent (Chronos in the classical variant), while the other involves all other space variables and time (Topos in the classical variant).

4. Energy and entropy

The global energy of the system is represented by one half of the sum of variances of all quantities describing the system state. In our case the quantities are all evaluated velocity components in all points in space. The space is always bounded and not all velocity components are measured. In PIV method typically we have a measuring plane with regularly distributed measuring point forming rectangular mesh. In all measuring points the 2 in-plane velocity components are evaluated for classical PIV, and 3 components in the case of stereo PIV technique. The eigenvalue λ_k^2 represent the *k*-th mode basic energy, while λ_k is the mode amplitude (see (16)). The basic energy is defined as a sum of variances of all velocity components appearing in the given case.

Information entropy, or the Shannon-Kolmogorov entropy, represents in general the average rate at which information is produced by a stochastic source of data. The measure of information entropy associated with each possible data value is the negative logarithm of the probability mass function for the value: $S = -\sum_i p_i \ln p_i$, see e.g. 18.

The global energy E could be evaluated as a sum of modes energies:

$$E(\mathbf{u}) = \frac{1}{2M}\int_X \int_T u_i(\mathbf{x},t)\overline{u_i(\mathbf{x},t)}\, d\mathbf{x}\, dt = \frac{1}{2M}\sum_{k=1}^{N}\lambda_k^2 , \tag{20}$$

The bar denotes complex conjugate, M is number of points in Euclidian space.

The temporal energy $E_t(t)$ indicates evolution the system global energy in time:

$$E_t(t) = \frac{1}{2M}\int_X u_i(\mathbf{x},t)\overline{u_i(\mathbf{x},t)}\, d\mathbf{x} = \frac{1}{2M}\sum_{k=1}^{N}\lambda_k^2 \left|\boldsymbol{\psi}_k(t)\right|^2 \tag{21}$$

The spatial energy $E_s(\mathbf{x})$ indicates distribution of the energy in space across the velocity components for the entire time interval *T*, it could be defined as follows:

$$E_s(\mathbf{x}) = \frac{1}{2M}\int_T u_i(\mathbf{x},t)\overline{u_i(\mathbf{x},t)}\, dt = \frac{1}{2M}\sum_{k=1}^{N}\lambda_k^2 \left|\boldsymbol{\varphi}_k(\mathbf{x})\right|^2 . \tag{22}$$

N is number of evaluated modes and it is expected to be big.

Please note that holds

$$E = \int_T E_t\, dt = \int_X E_s\, d\mathbf{x} . \tag{23}$$

The spatial energy is equal to TKE.

In the similar way the information entropies could be evaluated. For this purpose the probability of the individual mode appearance should be defined first.

Preprints (www.preprints.org) | NOT PEER-REVIEWED | Posted: 29 November 2018 doi:10.20944/preprints201811.0619.v1

As the Topoi and Chronoses are orthonormal, probability of appearance of the given k mode could be put to its mean dimensionless amplitude λ_k divided by sum of amplitudes of all modes.

$$p_k = \lambda_k \Big/ \sum_{k=1}^{N} \lambda_k \tag{24}$$

Temporal evolution and spatial distributions of the velocity deviation probability are defined by the modes weighting

$$\begin{aligned} p_{tk}(t) &= \lambda_k |\boldsymbol{\psi}_k(t)| \Big/ \sum_{k=1}^{N} \lambda_k |\boldsymbol{\psi}_k(t)|, \\ p_{sk}(\mathbf{x}) &= \lambda_k |\boldsymbol{\varphi}_k(\mathbf{x})| \Big/ \sum_{k=1}^{N} \lambda_k |\boldsymbol{\varphi}_k(\mathbf{x})|. \end{aligned} \tag{25}$$

Global entropy H, temporal entropy $H_t(t)$ and spatial entropy $H_s(\mathbf{x})$ with help of respective probabilities p are defined:

$$\begin{aligned} H &= -\frac{1}{\log N} \sum_{k=1}^{N} p_k \log p_k, \\ H_t(t) &= -\frac{1}{\log N} \sum_{k=1}^{N} p_{tk}(t) \log p_{tk}(t), \\ H_s(\mathbf{x}) &= -\frac{1}{\log N} \sum_{k=1}^{N} p_{sk}(\mathbf{x}) \log p_{sk}(\mathbf{x}). \end{aligned} \tag{26}$$

We introduce the normalizing factor "log N" in order to perform comparisons between different signal entropies. The global entropy H is zero if and only if only just one eigenvalue is nonzero, i.e., all the signal energy is concentrated in the first mode. As usual, in the opposite case, if all the eigenvalues are equal, i.e. the energy is equally distributed among the modes, then H takes its maximum value, namely 1. At intermediate states, H keeps increasing as the amplitudes spreads out uniformly on the eigenvalues. This function will be useful in hydrodynamics for a quantitative description of the increasing degree of complexity as the Reynolds number (or another dimensionless parameter characteristic of the system such as the Rayleigh number or an aspect ratio) gets higher and higher and the flow evolves toward a fully developed turbulent state and even beyond.

5. Example

As an example the case of wake behind an inclined flat plate will be shown. Instantaneous velocity fields in the flow-domain are acquired with high frequency (1 kHz) using Particle Image Velocimetry method, 4000 snapshots are available in a record. Only the two in-plane velocity components were evaluated.

The schematic view on the experimental setup is in Figure 1. The flat plate with rounded edges, thickness 2 mm and chord 100 mm is subjected to regular flow with velocity 10 m/s and angle of attack 7 degrees. The region in the wake is subjected to analysis, the trailing edge is located in the coordinate system origin. The experiment is described in details e.g. in [19].

Preprints (www.preprints.org) | NOT PEER-REVIEWED | Posted: 29 November 2018 doi:10.20944/preprints201811.0619.v1

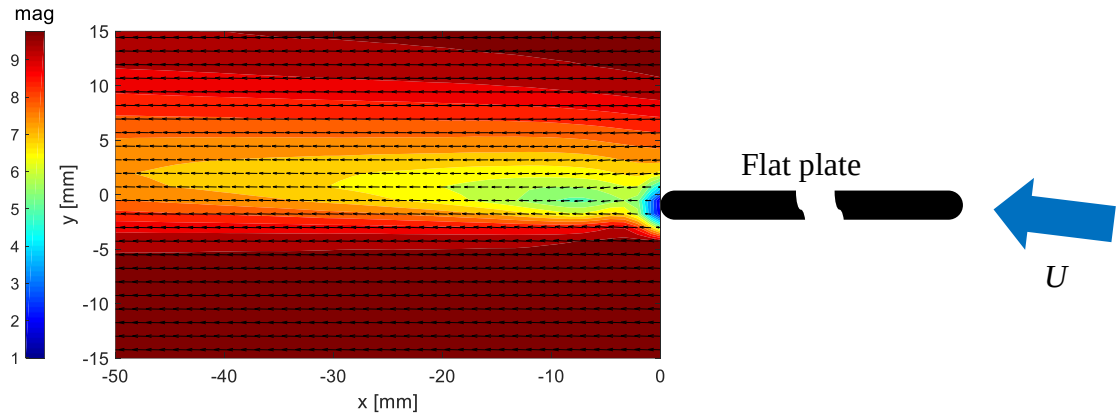

Figure 1. The mean velocity vectors and modulus distribution.

In Figure 1 the distributions of mean velocity vectors (arrows) and mean velocity magnitude (color) are shown. The magnitude scale is in [m/s]. To evaluate the velocity flow-field dynamics, variances of the velocity components in every point of space have been evaluated. In Figure 2 there is distribution of the evaluated sums of velocity components variances, covering a part of fluctuating kinetic energy in a given point. The "sumvar" scale (i.e. the sum of velocity components variances) is in [m^2/s^2].

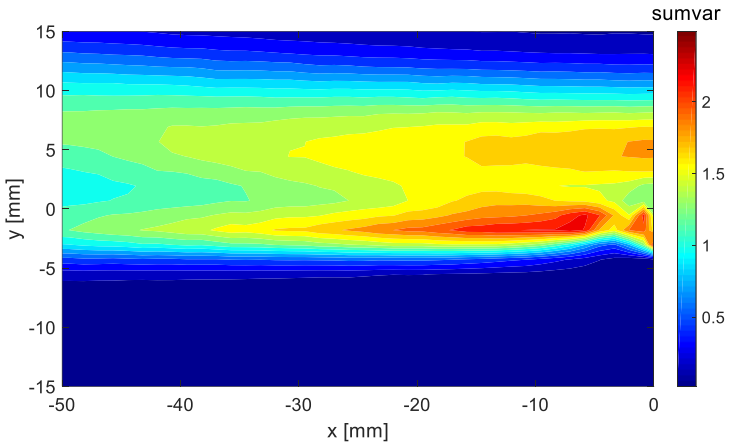

Figure 2. Sum of velocity components variances distribution.

The dynamic activity is maximal just behind the plate and secondary maximum is 5 mm above.

Now, the BOD method (see chapter 3.4) is applied on the set of 4 000 velocity distributions ("snapshots") available. The energetic modes are evaluated together with the other relevant characteristics, all over the 2340 modes, as this is number of Degrees of Freedom (see (15)), having the field 26 x 45 vectors with 2 components each.

First, the energy distributions over the modes are to be shown. In Figure 3 the Energy Fraction and Accumulated Energy are depicted graphically. Both graphs represent dimensionless quantities. The Energy Fraction indicates fraction of the total energy covered by the given mode. The first mode covers 9.7 % of the total kinetic energy, the second mode 8.7 %, the third 6.5 %, etc. The modes are ordered to have descending energy content. The Accumulated Energy shows the energy content of the first n modes in sum. For example the first 10 modes cover about 40 % of the total energy. This information is important for the correct choice of modes truncation threshold for the sake of the ROM purpose.

Preprints (www.preprints.org) | NOT PEER-REVIEWED | Posted: 29 November 2018 doi:10.20944/preprints201811.0619.v1

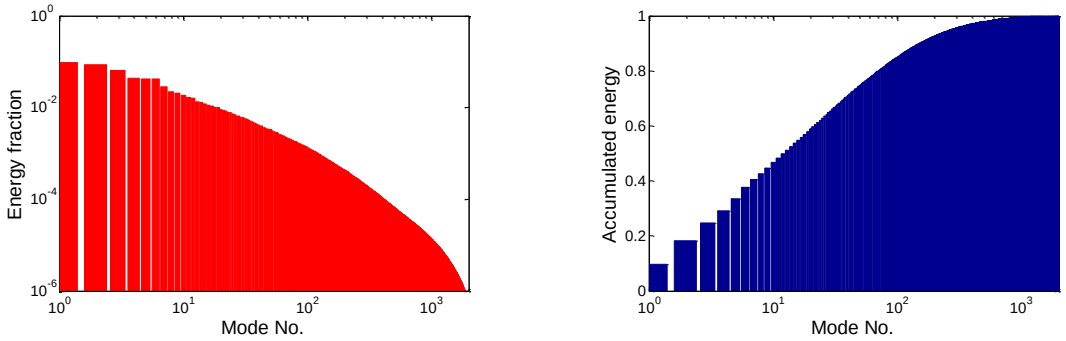

(**a**) (**b**)

Figure 3. Energy distribution over the modes: (**a**) Energy Fraction; (**b**) Accumulated Energy.

Please note that the Energy Fraction is represented in logarithmic coordinates, while Accumulated Energy is in semi-logarithmic representation.

Each energetic mode is represented by Topos, Chronos and amplitude (or energy). A few examples of modes are to be shown and commented. Please note that the Topos reflects flow topology represented by the vector-field regardless its amplitude, which could be virtually any, positive or negative. The Chronos is represented by a signal over the time *t*.

The first mode, containing 9.7 % of the total kinetic energy, is documented in Figure 4.

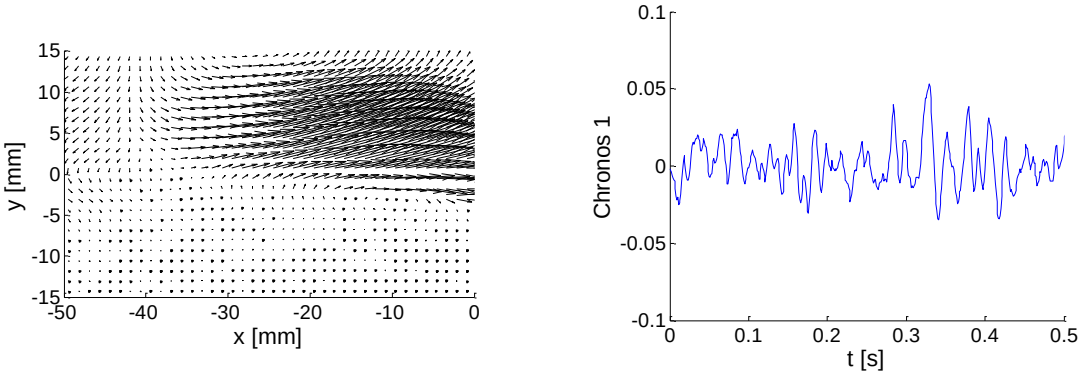

(**a**) (**b**)

Figure 4. Example of a BOD mode No. 1: (**a**) Topos; (**b**) Chronos.

The Topos (Figure 4a) is represented by intensive streamwise flow in the upper domain half, oscillation are negative and positive with low frequency defined by the corresponding Chronos (Figure 4b). Only part of the Chronos is shown to demonstrate the signal structure, whole Chronos covers the time range 0-4 s.

Next example is the mode No. 3 covering 6.5 % of the total kinetic energy. The Topos and Chronos are depicted in Figure 5.

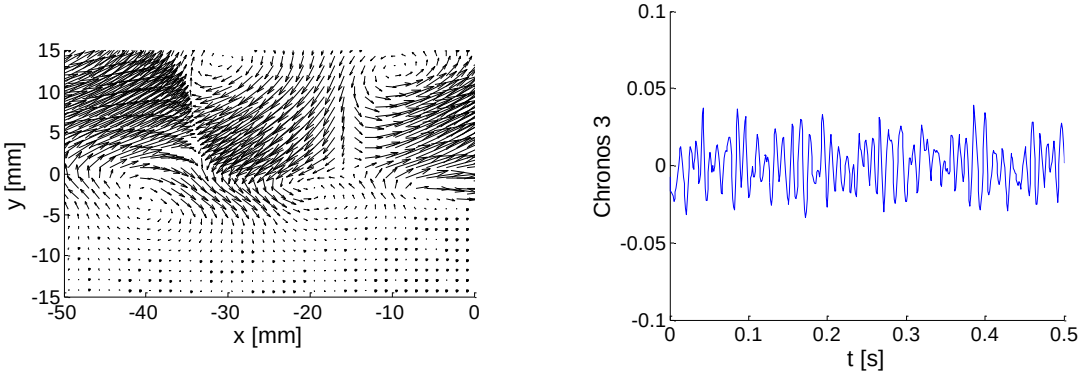

(**a**) (**b**)

Preprints (www.preprints.org) | NOT PEER-REVIEWED | Posted: 29 November 2018 doi:10.20944/preprints201811.0619.v1

Figure 5. Example of a BOD mode No. 3: (**a**) Topos; (**b**) Chronos.

Two rows of big vortices located in the upper half of the flow-field represent the corresponding Topos. The Chronos suggests higher frequency contents of pulsations in comparison with the mode 1.

The modes No. 5 and 6 are very similar to each other, see Figures 6 and 7. The Energy Fractions are 4.27 and 4.23 % of the total kinetic energy respectively, altogether these two modes contain 8.5 %. The Topoi represent a common flow pattern: vortex-street behind the plate, which is a periodical process both in space and time. The difference between the modes is in phase, the modes 5 and 6 are shifted both in space and time by ¼ of period. This means that the positions of vortices in Topoi are shifted in space, while Chronoses are shifted in time. The frequency is around 390 Hz, obviously much higher than in the preceding modes.

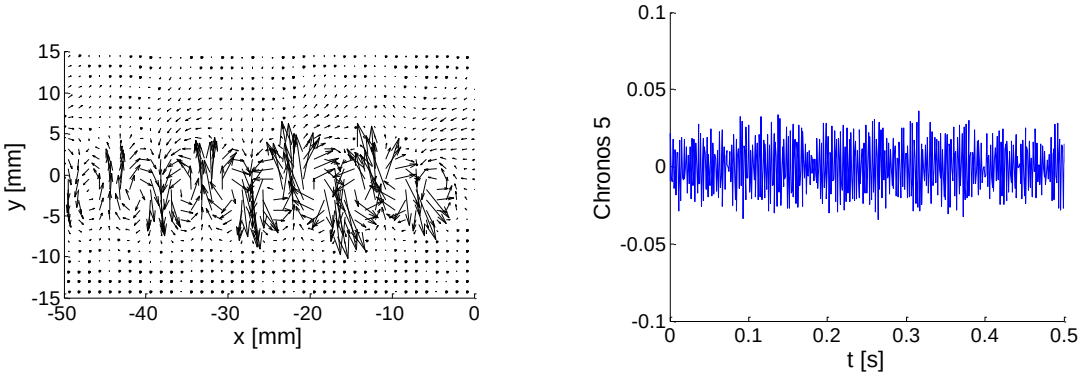

(**a**) (**b**)

Figure 6. Example of a BOD mode No. 5: (**a**) Topos; (**b**) Chronos.

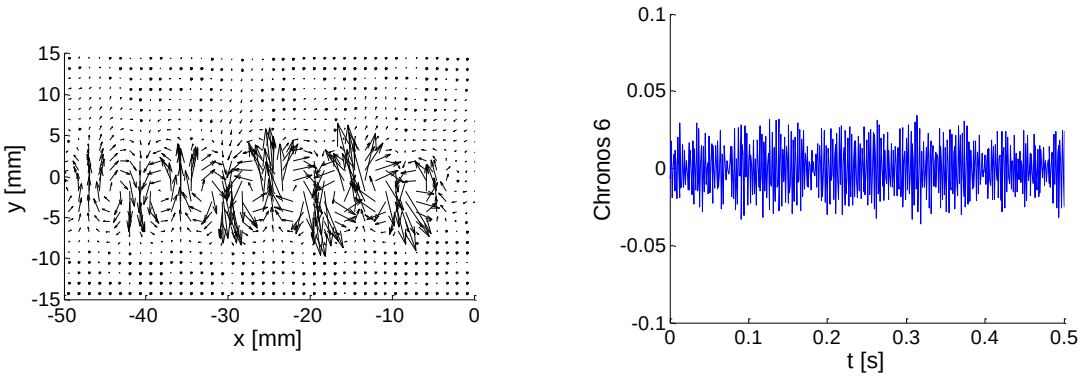

(**a**) (**b**)

Figure 7. Example of a BOD mode No. 6: (**a**) Topos; (**b**) Chronos.

The last example is the mode No. 7. Again, we could identify another configuration of the two rows of the counter-rotating vortices.

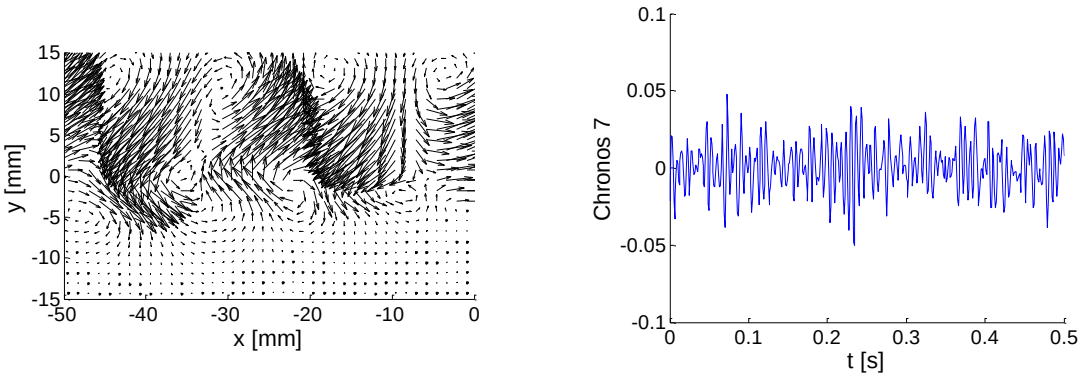

Preprints (www.preprints.org) | NOT PEER-REVIEWED | Posted: 29 November 2018 doi:10.20944/preprints201811.0619.v1

(**a**) (**b**)

Figure 8. Example of a BOD mode No. 7: (**a**) Topos; (**b**) Chronos.

Generally, the higher mode order, the lower energy, the smaller structures in Topos, the higher frequencies in Chronos. However if periodical structures are represented, the energy is higher and the mode order is lower.

Finally, the global energy and entropy distributions in space and time are evaluated (see chapter 4) for the given case. In Figure 9 there are distributions in space, while in Figure 10 distributions in time are presented.

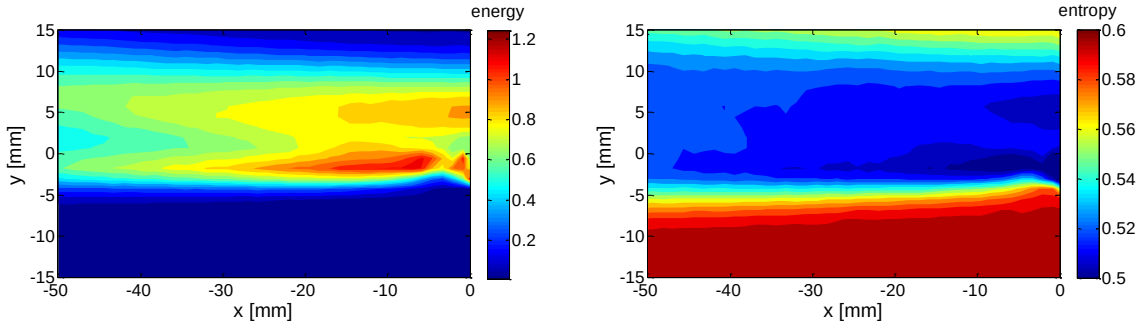

(**a**) (**b**)

Figure 9. Distributions in space: (**a**) energy distribution; (**b**) entropy distribution.

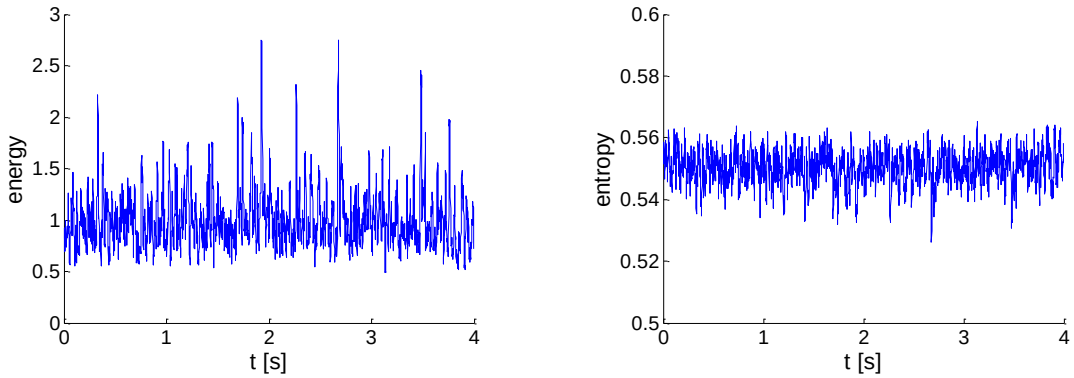

(**a**) (**b**)

Figure 10. Distributions in time: (**a**) energy distribution; (**b**) entropy distribution.

The global entropy was evaluated: $H = 0.550$. The normalization of temporal and spatial entropies makes the global entropy value the mean in space and time respectively.

The distributions of energy and entropy in space are close to be opposite to each other. In the wake region there is maximum of energy, while entropy is minimal. This means that the velocity variance in the wake could be linked to coherent structures namely. On the other hand the flow in lower half of the flow-field consists of low energy highly random structures. The randomness could come from the fact, that the low level signal is subjected to important relative random error of measurement. The distributions in time in Figure 10 indicate high randomly distributed peaks in energy signal, while entropy time evolution is relatively less disturbed.

Now, compare Figure 9a showing distribution of the energy in space with Figure 2 representing the sum of velocity components variances distribution. The distributions are identical, values of energy are half of values of the sum of velocity components variances. This is consistent with the energy definition (22). Evaluation of the energy distribution in space using BOD technique could be considered as a very expensive way, how to evaluate the energy distribution in space. However, the procedure could be used for evaluation of energy distribution connected with a specific BOD mode

Preprints (www.preprints.org) | NOT PEER-REVIEWED | Posted: 29 November 2018 doi:10.20944/preprints201811.0619.v1

or modes only. To demonstrate this feature the energy distributions linked to the 1st BOD mode have been evaluated and presented in Figure 11.

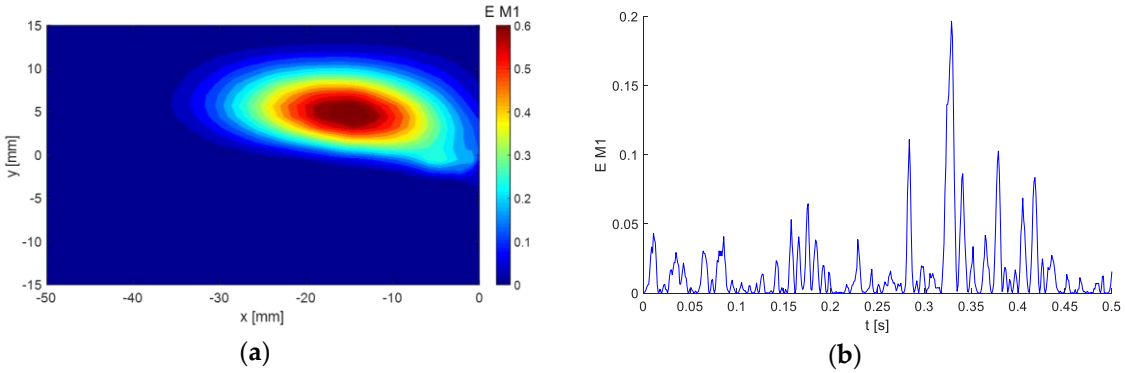

(**a**) (**b**)

Figure 11. Energy of the 1st BOD mode distributions: (**a**) in space; (**b**) in time.

The energy of the 1st mode is located in the upper part of the flow-field. The time evolution indicates very intensive bursts randomly distributed in time with calm periods (energy approaching 0) in between.

Very different energy distribution in time is in Figure 12b, where the two modes 5 and 6 representing vortex shedding process are involved (see Figures 6 and 7). The energy level is lower than for the BOD 1, however it is more uniform, no bursts are present. Resulting global energy is nearly the same. This behavior corresponds to quasi-periodical process. The energy is concentrated in the wake close to $y = 0$.

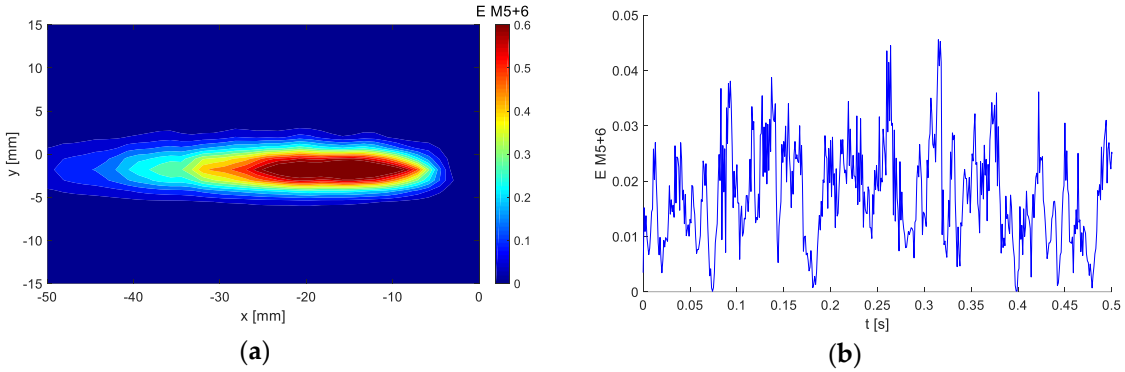

(**a**) (**b**)

Figure 12. Sum of energies of the 5th and 6th BOD modes distributions: (**a**) in space; (**b**) in time.

Generally, the energy could be decomposed on the basis of BOD modes.

6. Discussion

The BOD energetic modes represent dynamical content of the extended dynamical system under analysis. The modes are ordered in descending order, the energy decay rate is a key feature of the BOD representation of the system dynamics. The global entropy H could be used as an indicator of the modes decay rate.

To study the modes energy decay rate effect on the global entropy, the decay has been modelled numerically for low number of Degree of Freedom equal to 100. The energy fraction across the modes is supposed to be close to exponential decay. In Figure 13 the Energy Fraction decays and Accumulated Energy curves are shown with corresponding global entropies calculated with help of the formula (26).

Preprints (www.preprints.org) | NOT PEER-REVIEWED | Posted: 29 November 2018 doi:10.20944/preprints201811.0619.v1

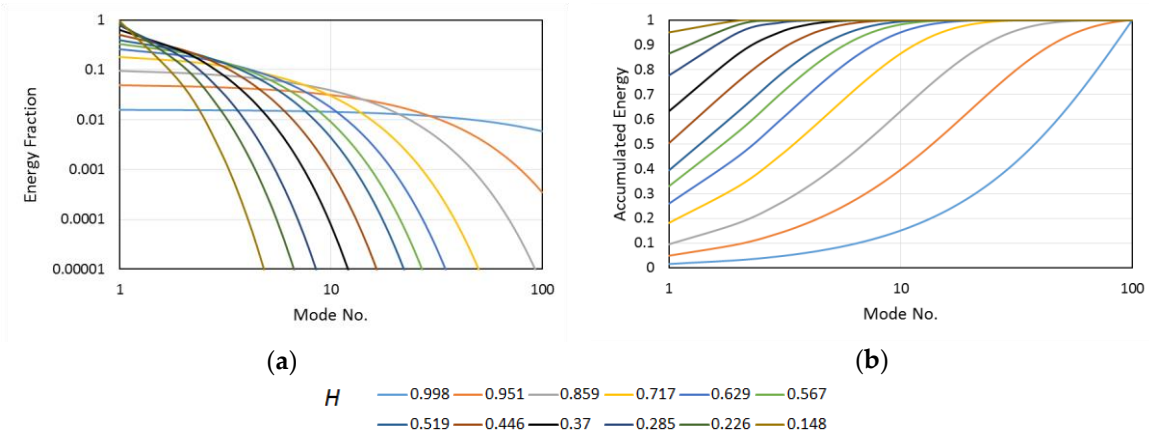

Figure 13. Simulated link between the global entropy and: (**a**) Energy Fraction; (**b**) Accumulated Energy.

The global entropy value ranges from the value of 0.148 up to 0.998. The value 0.998 means nearly even distribution of the energy over the modes resulting in nearly linear Accumulated Energy development. Lower global entropy value makes the convergence of the Accumulated Energy to 1 more effective. For the $H = 0.148$ the first mode covers the most of the system energy. Thus, the system dynamics could be modelled efficiently by single mode. Evaluation of a given dynamical system in context of ROM (see e.g. [20]) could be performed with help of the global entropy. However, this information is irrelevant in context of coherency and complexity of the given mode topology and/or its evolution in time. In general, the higher order of the mode, the lower its energy and the higher level of complexity.

In future the method of complexity of the individual BOD modes evaluation is to be addressed.

7. Conclusions

Definitions of energy and entropy are given in the paper in context of turbulent velocity field decomposition. The examples of distributions of energy and entropy both in space and time are shown. Generally, the entropy is higher for the low energy regions, where the random signal prevails. High energy structures are coherent as a rule.

The entropy is the factor determining the spatio-temporal data coherency. Global entropy measures coherency of the entire system. Temporal entropy shows distribution of the entropy over the time, while spatial entropy shows distribution of the entropy in space. This information together with energy distributions is helpful in physical interpretation of energetic modes.

Global entropy seems to be a good measure of the Reduced Order Modelling technique efficiency. Evaluation method of the individual modes coherency is to be developed in future.

Acknowledgement: This work was supported by the Grant Agency of the Czech Republic, project No. 17-01088S.

Conflicts of Interest: The author declares no conflict of interest.

References

1. Pope, S.B. Turbulent Flows. *Cambridge University Press*, **2000**.
2. Lumley, J.L. The structure of inhomogeneous turbulent flows. *Atm.Turb. and Radio Wave Prop.*, Yaglom and Tatarsky eds., Nauka, Moskva, **1967**, 166-178.
3. Aubry, N., Guyonnet, R., Lima, R. Spatiotemporal Analysis of Complex Signals: Theory and Applications. *Journal of Statistical Physics*, 64, Nos. 2/3, **1991**, 683-739.
4. Arnold, L. Stochastic Differential Equations: Theory and Applications. *Wiley & Sons*, **1974**.
5. Bendat, J.S., Piersol, A.G. Random Data: Analysis and Measurement Procedures. *Wiley & Sons*, **2011**.

6. Pearson, K. On lines and planes of closest fit to systems of points in space, *The London, Edinburgh, and Dublin Philosophical Magazine and Journal of Science*, **1901,** 2, No. 11, 559-572.
7. Hotelling, H. Analysis of a complex of statistical variables into principal components. *Journal of Educational Psychology*, **1933,** 24, No. 6, 417-441.
8. Kosambi D.D. Statistics in function space. *J. Ind. Math. Soc*., **1943**, 7, 76–88.
9. Loève, M. Nouvelles classes de lois limites. *Bull. Soc. Math. France*, **1945**.
10. Karhunen, K. Zur spektraltheorie stochastischer prozesse, *Ann. Acad. Sci. Fennicae*, AI, **1946**.
11. Pougachev, V.S. The general theory of correlation of random functions. *Izv. Akad. Nauk SSSR Ser. Mat*., **1953**, 17, Issue 5, 401–420.
12. Obukbov, A.M. Statistical description of continuous fields. *Tr. Geophys. Int. Akad. Nauk. SSSR*, **1954**, 24, 3-42.
13. Tropea, C., Yarin, A.L., Foss, J.F. eds. Handbook of Experimental Fluid Mechanics. *Springer*, **2007**.
14. Adrian, R.J., Christensen, K.T., and Liu, Z.C. Analysis and interpretation of instantaneous turbulent velocity fields. *Experiments in Fluids*, 29, No. 3, **2000**, pp. 275–290.
15. Lumley, J.L. Coherent structures in turbulence, Transition and Turbulence. (Ed. R.E.Meyer), *Academic Press, New York*, **1981**, 215-242.
16. Uruba, V. Decomposition methods in turbulence research. *EPJ Web of Conferences*, **2012**, 25, 01095.
17. Sirovich, L. Turbulence and the dynamics of coherent structures. *Quart. Appl. Math*., **1987**, 45, 561-590.
18. Shannon, C.E. A mathematical theory of communication. Bell Syst. Tech. J. **1948**, 27 379–423, 623–656.
19. Uruba, V., Procházka, P., Skála, V. On the structure of the boundary layer under adverse pressure gradient on an inclined plate. *Journal of Physics: Conference Series*, **2018**, 1101, Issue 1, Art. no. 012047.
20. Stankiewicz, W., Morzyński, M., Noack, B.R. & Tadmor G. Reduced order Galerkin models of flow around NACA-0012 airfoil, *Mathematical Modelling and Analysis*, **2008**, 13, No. 1, 113-122